

Fast neutron response of a ${}^6\text{Li}$ -loaded liquid scintillator

Masateru Hayashi^{*}

Department of Advanced Energy Engineering Science, Kyushu University

Kasuga, Fukuoka 816-8580, Japan

E-mail: teru@aees.kyushu-u.ac.jp

Yukinobu Watanabe¹, Daisuke Kaku¹, Hideki Nakashima¹, Kenshi Sagara²

¹*Department of Advanced Energy Engineering Science, Kyushu University*

Kasuga, Fukuoka 816-8580, Japan

²*Department of Physics, Kyushu University, Fukuoka 812-8581, Japan*

We have investigated the energy response of a ${}^6\text{Li}$ -loaded liquid scintillator to MeV neutrons. It consists of three ${}^6\text{Li}$ -glass scintillator plates inside a liquid organic scintillator BC-501A, which can detect selectively neutrons that lose the full energy in the BC-501A using a coincidence signal generated from the capture event of thermalized neutrons in the ${}^6\text{Li}$ -glass scintillators. The response functions were measured using 4.7, 7.2 and 9.0 MeV monoenergetic neutrons. The measured ones were compared with Monte Carlo calculations performed by combining the neutron transport code PHITS and the scintillator response calculation code SCINFUL. The experimental light output spectra were in good agreement with the calculated ones in shape. The energy dependence of the detection efficiency was reproduced by the calculation.

*International Workshop on Fast Neutron Detectors
University of Cape Town, South Africa
April 3 – 6, 2006*

^{*} Speaker

1. Introduction

Various types of fast neutron spectrometers (FNSs) have been proposed and used widely in experiments for nuclear physics and in a variety of application fields. It is a desirable feature for FNSs to have a single peak response to monoenergetic neutrons, particularly in the case where TOF methods are not available. A light output spectrum produced by monoenergetic neutrons in a typical organic or plastic scintillator forms a broad continuum because most of fast neutrons enter the scintillator and then escape after losing a variable fraction of their energy. If only the events corresponding to full energy deposition are selected, the detector response is expected to form a single peak with a modest efficiency for liquid or plastic scintillators. Full energy absorption scintillators based on this idea have so far been developed for FNSs: boron-loaded plastic [1,2], boron-loaded liquid scintillators [3] and neutron coincidence spectrometers combining the organic scintillator and the ${}^6\text{Li}$ -loaded glass scintillator plates [4,5,6]. Also there are other types of fast neutron scintillator detectors having peaked responses, *e.g.*, deuterated organic scintillators [7] and Black Neutron Detectors consisting of large volume scintillator [8].

In the present work, we pay attention to a liquid scintillator with ${}^6\text{Li}$ -loaded glass scintillator, which will be hereinafter called as ${}^6\text{Li}$ -loaded liquid scintillator. The different decay times of the liquid scintillator and the Li-glass scintillator allow pulse shape discrimination methods to be used to separate the events due to proton recoil, ${}^6\text{Li}$ -capture, and γ -rays. This is of great benefit for a more specific identification of the full-energy absorption event due to elimination of γ -rays background. Although some spectrometers of this type have been developed and applied to fast neutron spectroscopy [4,5,6], few comparisons of the measured responses with Monte Carlo calculations have been reported in details. In the present work, light output spectra are measured for monoenergetic neutrons in the MeV region and compared with Monte Carlo calculations.

2. ${}^6\text{Li}$ -loaded liquid scintillator

The scintillator (Bicron Corporation Model 5FNS5/5(2)L) used in the present work consists of three ${}^6\text{Li}$ -glass scintillator plates (Bicron Corporation Model GS20, 1.5 mm thick and 6.6 wt% ${}^6\text{Li}$) in a liquid organic scintillator (BC-501A 12.7 cm in diameter and 12.7 cm long), which is coupled to two photomultiplier tubes (PMT) as shown in Fig.1.

The principle of this fast neutron spectrometer is as follows. A fast neutron incident on the BC-501A loses its energy through multiple scattering from hydrogen nuclei and becomes a thermal neutron within the BC-501A. All recoil protons are produced within a very short period of time, typically several tens of nsec. Because they appear in a short time compared with the pulse shaping time, the light from the recoil protons is summed and a single light output pulse is produced. On the other hand, the thermalized neutron diffuses in the BC-501A and will be eventually captured by ${}^6\text{Li}$ nuclei in the Li-glass scintillators before escaping from the BC-501A because of the large capture cross-section (940 barns). The neutron capture results in production of a pair of triton and α whose total kinetic energy is 4.78 MeV, and they deposit their energy

locally in the Li-glass and give rise to a second light pulse. The mean diffusion time corresponding to the time difference between the first and second light pulses is in the order of μsec . By making a gate signal from the associated second pulse, the spectrometer can detect selectively neutrons that deposit the full energy in the BC-501A. Thus, the pulse height spectrum to a monoenergetic neutron is expected to have a single peak.

Figures 2 and 3 show the block diagram of electronics and the timing chart for the present measurement. The dynode signals from both PMTs were sent to a preamplifier and then processed by conventional NIM electronics. The energy signal amplified by a delay line amplifier was delayed to be coincident with the arrival of a capture gate signal corresponding to an event of full energy deposition. The capture gate signal was created after the events due to prompt proton recoil, ${}^6\text{Li}$ -capture, and γ -background were separated respectively from the output pulse signals using a method of pulse shape discrimination (PSD).

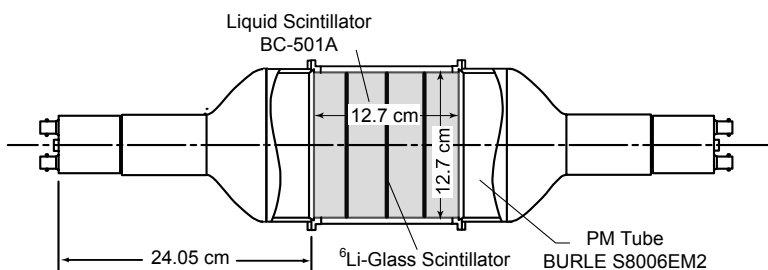


Figure 1: Schematic diagram of the ${}^6\text{Li}$ -loaded liquid scintillator

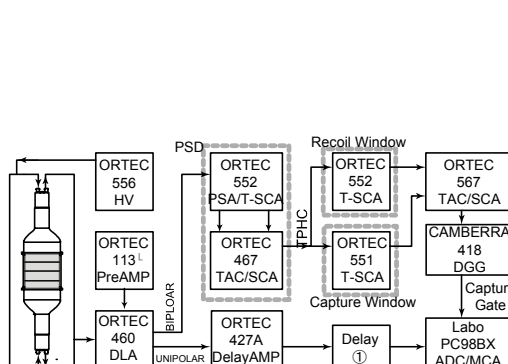


Figure 2: Block diagram of electronics

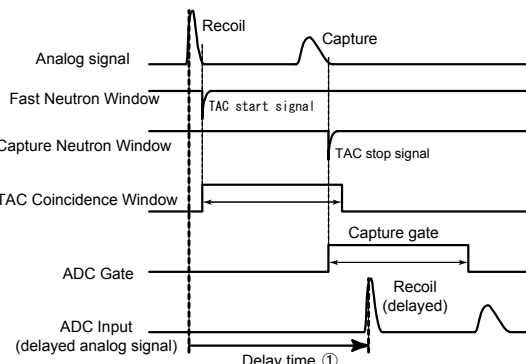


Figure 3: Timing chart of pulse processing

3. Experimental procedure

Monoenergetic neutrons in the MeV region were obtained from the ${}^2\text{H}(\text{d},\text{n}){}^3\text{He}$ reaction using deuterons from the tandem Van de Graaf accelerator at Kyushu University Tandem Laboratory, irradiating a gas cell target filling D_2 gas of 1 atm [9]. The detector was placed 2 m downstream from the neutron source at 0° relative to the incident deuteron beam, so that

neutrons were incident from a direction perpendicular to the side of the cylindrical scintillator. Background measurements were carried out by inserting an iron shadow bar between the neutron source and the detector in order to eliminate the influence of room-scattered neutrons. The energy calibration of light output spectrum was established using ${}^{137}\text{Cs}$ and ${}^{60}\text{Co}$ gamma sources. The position of the Compton edge was determined by a method of Dietze and Klein [10] considering the influence of detector resolution.

4. Results and discussion

A preliminary experiment was carried out in order to examine the basic operation performance of the present spectrometer using 7.2 MeV neutrons. First of all, we have confirmed whether the light pulses produced in the BC-501A and the Li-glass scintillators and those due to background γ -rays are distinguished readily using the conventional PSD method. The result is shown as a two-dimensional plot in Fig. 4. It is seen that these three events are well separated and the recoil and capture windows for the PSD output signals can be established using the two SCAs following the PSD circuit in Fig.2. However, it should be noted that selection of the signals due to ${}^6\text{Li}$ will become difficult for neutron energies over 9 MeV because signals from reactions on carbon in the BC501A, *i.e.*, ${}^{12}\text{C}(\text{n},\alpha)$ and ${}^{12}\text{C}(\text{n},\text{n}'3\alpha)$, are expected to show similar pulse shapes.

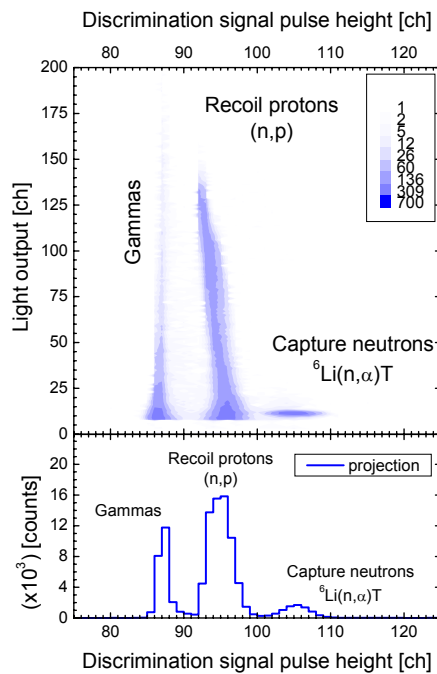


Figure 4: Two-dimensional plot of the light output from the PMT dynode and the PSD pulse height and the projection on the PSD axis

Next, we measured the mean capture delay time corresponding to the time differences between the recoil pulse produced in the BC501A and the capture pulse from ${}^6\text{Li}$ -glass scintillators. The result is shown in Fig.5. The distribution of the time differences contains the nearly flat portion due to chance coincidences. The capture gate time was determined to be 5 μsec in order to achieve a rather good signal to noise ratio, although the mean capture lifetime is about 11 μsec .

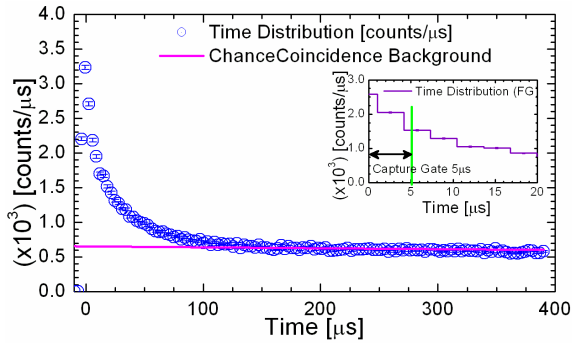


Figure 5: Distribution of the time differences between the recoil and capture pulses. The red line corresponds to chance coincidence event.

Light output spectra of the ${}^6\text{Li}$ -loaded liquid scintillator were measured using 4.7, 7.2 and 9.0 MeV monoenergetic neutrons. In Fig.6, the experimental spectra are shown by open circles with statistical errors. Although a single peak corresponding to full energy deposition is clearly observed for three incident energies, it is not Gaussian-shaped and the width is rather broad. This degraded energy resolution may be caused by the inherent nonlinear characteristic of organic scintillators as discussed in the previous works on ${}^6\text{Li}$ -loaded or boron-loaded scintillators [11]. The experimental light output spectra were compared with the calculation using the SCINFIL code [12] based on a Monte Carlo method. In the SCINFUL calculation, the response function was obtained by extracting only the events that incident neutron slows down in the BC-501A scintillator and its energy becomes lower than a given cut-off energy. The cut-off energy was set to be 0.1 eV, because the fraction of thermalized neutrons to incident neutrons was saturated around this cut-off energy. Since the absorption of thermal neutrons by the Li-glass cannot be considered in the SCINFUL code, the calculated efficiency is normalized to the experimental one in Fig.6. The calculation results showed fairly good agreement with the measured ones, except at low light outputs for 4.7 and 7.2 MeV. The discrepancy may be due to the influence of chance coincidence. There is a rise in the calculated light output spectra at low pulse amplitude for two incident energies of 7.2 and 9.0 MeV, which is caused by inelastic scattering of fast neutrons from carbon in BC-501A.

The detection efficiency can be obtained by integrating the pulse height spectrum in Fig. 6 and dividing the integral counts by the number of incident neutrons. However, it was difficult to derive the absolute efficiency because we met a problem on the absolute neutron flux

measurement. Therefore, we obtained the relative efficiency from the SCINFUL response normalized to the experimental one in Fig.6, so that influence of chance coincidence is eliminated and the pulse height threshold is extended to zero. Next, the absolute detection efficiency was estimated by neutron transport Monte Carlo calculations using the PHITS code [13] with JENDL-3.2 nuclear data library [14]. The ${}^6\text{Li}$ capture rate was calculated as a function of time after neutron incidence and was integrated over the capture gate width (5 μsec) used in the measurement in order to derive the detection efficiency. The energy dependence is shown by the solid curve in Fig. 7. It decreases monotonically as the neutron energy decreases, ranging from 4.7 % at 1 MeV to 0.6 % 10 MeV. The values are more or less same as those for the other ${}^6\text{Li}$ -loaded [4,6] and boron-loaded scintillators [2,3], although they depend on the size and detailed design of the scintillator. The normalized experimental values are compared with the calculated curve in Fig. 7. The energy dependence of the experimental detection efficiencies is reproduced by the calculation.

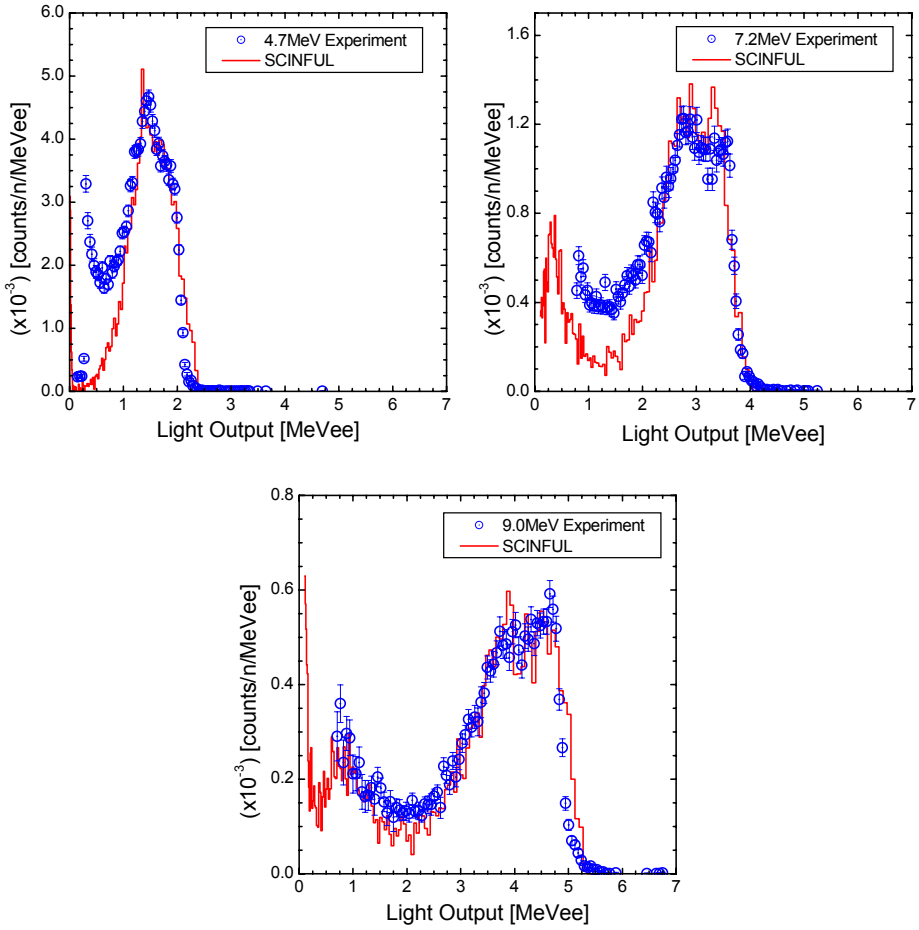


Figure 6: Comparisons between experimental response and functions and those calculated by the SCINFUL code.

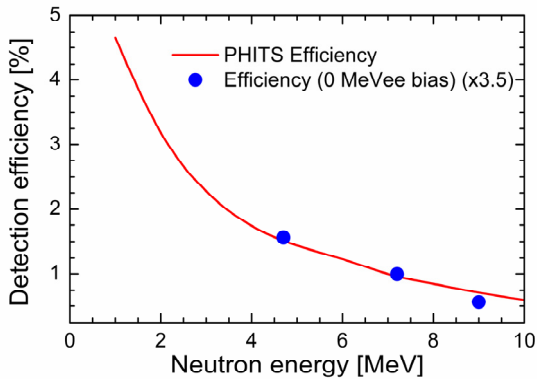


Figure 7: Neutron energy dependence of detection efficiency. The experimental efficiencies shown by solid circles are normalized to the calculated one at 7.2 MeV. The normalization factor is denoted in the figure.

POS (FENDA 2006) 046

5. Concluding remarks

The energy response of the ${}^6\text{Li}$ capture-gated fast neutron spectrometer to MeV neutrons was investigated from both the measurement and the Monte Carlo calculation. The response functions were measured using 4.7, 7.2 and 9.0 MeV monoenergetic neutrons. The measured ones were compared with those calculated by combining the neutron transport code PHITS and the scintillator response calculation code SCINFUL. The calculated response functions showed good agreement with the measured ones in shape and the PHITS calculation reproduced the energy dependence of the relative detection efficiency.

The present investigation has confirmed that this spectrometer has the broad single-peak response with modest efficiency in the MeV range. Here we remark briefly some limitations and improvements on the present fast neutron spectrometer and its preferable applications. First, it will be most suitable in the MeV neutron energy range, because selection of the signals from ${}^6\text{Li}$ capture event by means of the pulse shape discrimination method will be limited for energies above 9 MeV from the reason mentioned in sect. 4. Second, counting rates will be limited because of the relatively long capture gate width of the order of μsec . Increase of the ${}^6\text{Li}$ content or increase of the number of the Li glass plates is expected to improve the detection efficiency and to shorten the mean capture lifetime. The latter will allow one to use a shorter capture gate width and to relax the limitation of counting rates. Also, application of recent digital data acquisition techniques to this spectrometer may lead to a possible improvement in pulse shape discrimination. Finally, this type of the spectrometer would be used effectively for measurements of neutrons with low intensity, such as spontaneous-fission neutrons from minor actinides such as Pu and Cm isotopes and low-level environmental neutrons associated with estimation of single-event upsets in semiconductor memories.

In future work, we plan to carry out an additional response measurement to neutrons with energies below 4 MeV and to determine the absolute efficiency experimentally for the practical

use. Together with the measurement, further Monte Carlo calculations will be necessary for optimization of the detector parameters such as the ${}^6\text{Li}$ -content.

Acknowledgements

The authors would like to thank the staff of the Kyushu University Tandem Accelerator Laboratory for their assistance during the experiments. M.H. is grateful to Prof. J. Blomgren for kindly providing financial support to participate in FNDA2006 during his stay in the Department of Neutron Research, Uppsala University.

References

- [1] W.C. Feldman, G.F. Auchampaugh and R.C. Byrd, *A novel fast-neutron detector for space applications*, Nucl. Instr. and Meth. **A306** (1991) 350.
- [2] E.A. Kamykowski, *Comparison of calculated and measured spectral response and intrinsic efficiency for a boron-loaded plastic neutron detector*, Nucl. Instr. and Meth. **A317** (1992) 559.
- [3] T. Aoyama, K. Honda, C. Mori, K. Kudo and N. Takeda, *Energy response of a full-energy-absorption neutron spectrometer using boron-loaded liquid scintillator BC-523*, Nucl. Instr. and Meth. **A333** (1993) 492.
- [4] J.B. Czirr and G. L. Jensen, *A neutron coincidence spectrometer*, Nucl. Instr. and Meth. **A284** (1989) 365.
- [5] S.E. Jones, E.P. Palmer, J.B. Czirr, D.L. Decker, G.L. Jensen, J.M. Thorne, S.F. Tayer and J. Rafelski, *Observation of cold nuclear fusion in condensed matter*, Nature **338** (1989) 737.
- [6] J.B. Czirr and G. L. Jensen, *A compact neutron coincidence spectrometer, its measured response functions and potential applications*, Nucl. Instr. and Meth. **A349** (1994) 532.
- [7] F.D. Brook, W.A. Cilliers, B.R.S. Simpson, F.D. Smit, M.S. Allie, D.T.L. Jones, W.R. McMurray and J.V. Pilcher, *Deuterated anthracene spectrometer for 5-30 MeV neutrons*, Nucl. Instr. and Meth. **A270** (1988) 149.
- [8] W.P. Poenitz, *The black neutron detector*, Nucl. Instr. and Meth. **109** (1973) 413.
- [9] Y. Watanabe, Y. Matsuoka, H. Nakamura, H. Nakashima, N. Ikeda and K. Sagara, *Development of quasi-monoenergetic neutron source using the ${}^1\text{H}({}^{13}\text{C},n)$ reaction*, Engineering Science Reports, Kyushu Univ. Vol. **23**, No.3 (2001) 285.
- [10] G. Dietze and H. Klein, *Gamma-calibration of NE213 scintillation counters*, Nucl. Instr. and Meth. **193** (1982) 549.
- [11] G.J. Knoll, *Radiation Detection and Measurement, Third ed., Chap.15*, John Wiley & Sons, New York 2000.

- [12] J.K. Dickens, *SCINFUL*, ORNL-6452 (1988).
- [13] H. Iwase, K. Niita and T. Nakamura, *Development of general-purpose particle and heavy ion transport code*, J. Nucl. Sci. and Technol., **39** (2002) 1142.
- [14] T. Nakagawa, K. Shibata, S. Chiba, T. Fukahori, Y. Nakajima, Y. Kikuchi, T. Kawano, Y. Kanda, T. Ohsawa, H. Matsumoto, M. Kawai, A. Zukeran, T. Watanabe, S. Igarasi, K. Kosako, T. Asami, *Japanese Evaluated Nuclear Data Library version 3 revision-2: JENDL-3.2*, J. Nucl. Sci. and Technol., **32** (1995) 1259.